Framing Anomaly in Lattice Chern-Simons-Maxwell Theory

Ze-An Xu and Jing-Yuan Chen
Institute for Advanced Study, Tsinghua University, Beijing, 100084, China

(Received 8 February 2026; revised 12 July 2026; accepted 7 October 2026; published 4 November 2026)

Framing anomaly is a key property of $(2+1)d$ chiral topological orders, for it reveals that the chirality is an intrinsic bulk property of the system, rather than a property that requires a boundary between two systems. Understanding framing anomaly in lattice models is particularly interesting, as concrete, solvable lattice models of chiral topological orders are rare. In a previous work [Z.-A. Xu and J.-Y. Chen, J. High Energy Phys. 08 (2025) 062.], we defined and solved the U(1) Chern-Simons-Maxwell theory on spacetime lattice, showing its chiral edge mode and the associated gravitational anomaly on boundary. In this Letter, we show its framing anomaly in the absence of boundary by computing the expectation of a lattice version of the modular T operator in the ground subspace on a spatial torus, from which we extract that $\langle T\rangle$ has a universal phase of $-2\pi/12$ as expected: $-2\pi/8$ from the Gauss-Milgram sum of the topological spins of the ground states, and $2\pi/24$ from the framing anomaly. We can also extract the $2\pi/24$ framing anomaly phase alone from the full spectrum of T in the ground subspace by computing $\langle T^m\rangle$. This pins down the last and most crucial property required for a valid lattice definition of U(1) Chern-Simons theory.

DOI: 10.1103/hyz3-3kxh

Introduction—Chern-Simons theory is a landmark in the formal development of quantum field theory [1,2], and is the effective theory that describes the quantum Hall effect [3]. Among its fascinating topological properties, one key characterization of a Chern-Simons theory is its *chirality*.

Chirality usually manifests in the form of gapless chiral edge modes, as has been observed in thermal Hall measurements [4]. Nonetheless, edge modes and thermal Hall conductivity are only definable as *relative* notions between two systems on the two sides of a boundary [5]. Meanwhile, it is conceptually important that chirality is an intrinsic bulk property of a system. (For comparison, electric Hall conductivity is an intrinsic bulk property, and since the early years, this understanding has played an important role in the development of the theory of the quantum Hall effect, e.g., [6].) In the absence of boundary, chirality manifests itself as a *framing anomaly* [2], which suggests the phase of the partition function has a dependence, in units of $2\pi c_-/24$, on the global choice of a basis of tangent vectors (a frame) over the spacetime, where c_- is the *chiral central charge* of the theory.

Associated to this, the modular T operator (see Fig. 1) acts on the ground subspace of a spatial torus as [7]

$$T = e^{-i2\pi(h-c_-/24)}, \tag{1}$$

where h is the operator measuring the conformal weight of a ground state, and $2\pi c_-/24$ is the framing anomaly. h and c_- are not entirely independent. For a bosonic topological order, the Gauss-Milgram formula reads [8,9]

$$\sum_{\text{gnd states}}^{N} e^{i2\pi h_n} = \sqrt{N} e^{i2\pi c_-/8}. \tag{2}$$

In particular, for bosonic U(1) Chern-Simons of even level-k, the ground states are labeled by $n \in \mathbb{Z}_{N=|k|}$, with purely imaginary $i2\pi h_n = i\pi n^2/k$ being the topological spin, and $c_- = \mathrm{sgn}(k)$. For fermionic systems, it is easy to see the modular T operator (Fig. 1) is only defined when the fermions obey *periodic* boundary conditions across the x direction, and in particular for U(1) Chern-Simons of odd level k, the periodic boundary condition makes the ground state topological spins $i2\pi h_n = i\pi(n+1/2)^2/k$ [10–12] in Eq. (2) (see Supplemental Material [13] for explanation), yielding the same right-hand side.

Solvable lattice models have played an important role in the development of the subject of topological order. However, most of the systematically constructed lattice models were for theories that are gappable on the boundary,

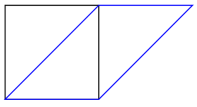


FIG. 1. Our convention of modular T operator *actively* brings the values of the fields at (x, y) to $(x + yL_x/L_y, y)$. (In the literature the convention is often passive.)

Published by the American Physical Society under the terms of the Creative Commons Attribution 4.0 International license. Further distribution of this work must maintain attribution to the author(s) and the published article's title, journal citation, and DOI. Funded by SCOAP³.

hence nonchiral [14]. Concrete, solvable models for chiral topological orders are very rare (an important example is [9]). Particularly, the lattice realization of chiral U(1) Chern-Simons has been a problem of interest for decades. Recently, by carefully putting together existing but scattered ideas, U(1) Chern-Simons-Maxwell theory has been defined on a lattice (with the Maxwell term needed for fundamental reasons) [15,16] and analytically solved. [A lattice model for SU(N) Chern-Simons-Yang-Mills has also been constructed by generalizing the U(1) case via higher category theory [17,18], though the SU(N) case is not analytically solvable.] The chiral edge mode and the associated gravitational anomaly on the boundary have been solved for in [16], showing the lattice model is indeed chiral. But it will be much more interesting if we can show the celebrated framing anomaly on the lattice *in the absence of boundary*. This will not only pin down the last key requirement from a successful lattice realization of U(1) Chern-Simons, but also provide an important example of a UV-complete study of the framing anomaly.

More broadly speaking, the general motivation of our program to realize Chern-Simons, the framing anomaly, and other formal aspects of quantum field theories on the lattice [17] is to make everything regularized in an explicit manner (and it is nontrivial to show that this is indeed possible) and hence more assessable.

In this Letter, we will define a spacetime lattice realization of the modular T operator acting on a spatial torus, and evaluate its expectation in the ground subspace of the lattice Chern-Simons-Maxwell theory. We will find, as expected, that

$$\langle T\rangle = \frac{e^{-i2\pi\,\mathrm{sgn}(k)(1/8-1/24)}}{\sqrt{|k|}}\, e^{-\alpha L^2+\cdots}, \tag{3}$$

where the first fraction is the universal contribution from Eq. (1) averaged over the ground states using Eq. (2) (or its fermionic counterpart), while in the second factor L^2 is the size of the spatial torus with α a nonuniversal complex number that can be removed by adding local counterterm to the definition of T (the L^2 scaling is because T is an extensive operator defined over the spatial torus), and "$\cdots$" represents finite size effects that vanish as $L\to\infty$.

We can also separate the $1/24$ framing anomaly contribution from the $-1/8$ Gauss-Milgram sum contribution by evaluating a lattice realization of $\langle T^m\rangle$ for $m\in\mathbb{Z}_+$—which can be recognized as a *higher central charge* calculation [19,20]—in order to extract the full spectrum of T in the ground subspace. The result indeed agrees with Eq. (1) for both bosonic and fermionic U(1) Chern-Simons (see End Matter).

Lattice Chern-Simons-Maxwell theory—We first review the Chern-Simons-Maxwell theory on a spacetime cubic lattice of Euclidean signature. The path integral reads [15,16]

$$\begin{aligned} Z = &\left[\prod_{\text{link } l}\int_{-\pi}^{\pi}\frac{dA_l}{2\pi}\right]\left[\prod_{\text{plaq}\,p}\sum_{s_p\in\mathbb{Z}}\right]\left[\prod_{\text{cube } c}\int_{-\pi}^{\pi}\frac{d\lambda_c}{2\pi}\,e^{i\lambda_c ds_c}\right]\\ &\times\exp\left\{\frac{ik}{4\pi}\sum_c[(A\cup dA)_c-(A\cup 2\pi s)_c-(2\pi s\cup A)_c]\right.\\ &\left.-\frac{1}{2e^2}\sum_p F_p^2\right\}. \end{aligned} \tag{4}$$

The second line is the lattice Chern-Simons term of level k [21,22] which we will explain soon. The last line is the Maxwell term, which is needed for *fundamental* reasons as explained in [15,16,21], with e^2 the Maxwell coupling in units where the lattice length is set to 1.

The dynamical U(1) gauge connection is $A_l\in(-\pi,\pi]$ on each lattice link l. The gauge flux around each plaquette p takes the "Villainized" form [21,23,24] (see Ref. [16] for an intuitive interpretation and [17] for the mathematical exposition),

$$F_p := dA_p - 2\pi s_p \in\mathbb{R}, \tag{5}$$

where dA_p is the lattice curl of A_l, and $s_p\in\mathbb{Z}$ is an independent dynamical variable, the "Dirac string" threading through p. Note A_l is not apparently 2π-periodic in F_p; rather, F_p has a one-form $\mathbb{Z}$ gauge invariance,

$$A_l\mapsto A_l+2\pi m_l,\qquad s_p\mapsto s_p+dm_p,\qquad m_l\in\mathbb{Z}, \tag{6}$$

and our restriction $A_l\in(-\pi,\pi]$ fixes this gauge. The Dirac monopole number inside a cube c is given by the lattice divergence $dF_c/2\pi=-ds_c\in\mathbb{Z}$, satisfying Dirac quantization. We have forbidden the monopoles by a Lagrange multiplier field $e^{i\lambda c}\in\mathrm{U}(1)$ [21,24]. But over a noncontractible surface, $\sum_p F_p=-2\pi\sum_p s_p\in 2\pi\mathbb{Z}$ can still be a Dirac quantized nonzero total flux, as is desired for a U(1) gauge theory.

The cup product in the lattice Chern-Simons term is defined as Fig. 2, which satisfies the Leibniz rule under lattice exterior derivative d. Thanks to this lattice Leibniz

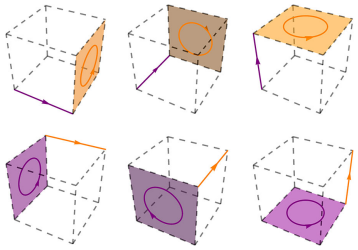


FIG. 2. Top: cup product $(X\cup Y)_c$ for a lattice one-form X and two-form Y on a cube c is a sum of three terms, each with the X value on a purple link multiplied to the Y value on an associated orange plaquette. Bottom: $(Y\cup X)_c$ is a different sum of three terms.

rule, in the absence of spacetime boundary, the model has gauge invariance under $A_l \mapsto A_l + d\phi_l$ (accompanied by suitable transformation of λ_c) for arbitrary $\phi_v \in \mathbb{R}$ on each vertex v. Furthermore, A_l (and hence ϕ_v) should be effectively 2π-periodic in the sense of Eq. (6). We can check the path integral is invariant under Eq. (6) if and only if $k \in 2\mathbb{Z}$—this is the lattice origin of the level quantization of the bosonic Chern-Simons term [21,22]. In this Letter we will not consider spacetime boundary, but a careful treatment of the boundary can be found in [16]. Also, the Chern-Simons term has some global symmetries and associated anomalies (see Ref. [22]) that are not altered by the inclusion of the Maxwell term.

When k is odd, under Eq. (6), the partition function has a sign ambiguity. This ambiguity can be canceled by including in the path integral an extra fermionic path integral $z_\chi[s \bmod 2]$, which is a functional of $s_p \bmod 2$ and takes value ± 1 [25], that depends on spin structure (fermion boundary condition) data [26]. The construction of z_χ on a cubic lattice [21] is reviewed in Supplemental Material [13]. This is the level quantization of fermionic Chern-Simons.

Lattice modular T operator—Consider a spatial torus with $L \times L$ lattice vertices. $\mathbf{Tr}\, e^{-\beta H}$ is constructed by the path integral Z_{T^3} over a three-torus $\mathrm{T}^3 = S^1 \times S^1 \times S^1$ with $L \times L \times \beta$ vertices. In [16] we have shown $Z_{\mathrm{T}^3} = |k| \exp(-\beta L^2 \epsilon_0 + \cdots)$, where $|k|$ is the desired ground state degeneracy on the spatial torus, ϵ_0 is some nonuniversal real-valued ground state energy density that can be removed by local counterterm, and "$\cdots$" are finite size effects that vanish exponentially in βL^2. Now, our task is to define the modular T operator on the spacetime lattice and evaluate $\mathbf{Tr}(T\, e^{-\beta H})$ as a lattice path integral.

First, $e^{-\beta H}$ before taking the trace is constructed by the path integral over $S^1 \times S^1 \times I$ of size $L \times L \times \beta$, as a function of the A and s fields on the $\tau = 0$ and the $\tau = \beta$ boundaries; see the lower part of Fig. 3. Then, the modular T operator is constructed as in the upper part of Fig. 3, with two layers of cubes in the τ direction glued in a twisted manner as shown, creating some triangular shaped plaquettes in between. To take the trace, as shown in Fig. 3, the square grid at the bottom of the lattice T operator is glued to that at the $\tau = \beta$ top layer of $e^{-\beta H}$, while the square grid at the top of the T operator is glued to that at the $\tau = 0$ bottom layer of $e^{-\beta H}$. (By "glue" we mean the A_l and s_p on the grids being identified are integrated or summed over.) The closed manifold thus created, which we denote as $\mathcal{T}$, is no longer a three-torus because a loop running across the x direction becomes contractible; see Supplemental Material [13].

How are the lattice Chern-Simons and Maxwell terms defined on those special layers of lattice cells in the modular T operator? It turns out, we can modify the cup product on the two special layers of cubes in T as Fig. 4, and find the lattice Leibniz rule and hence the gauge

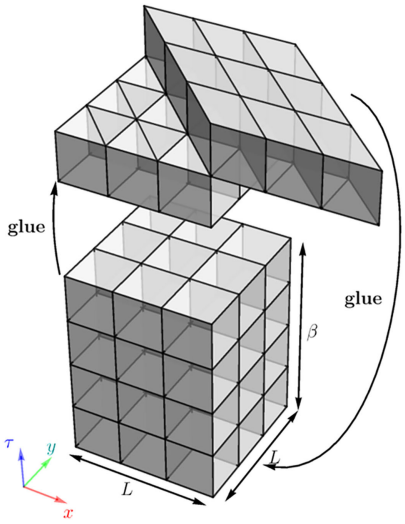


FIG. 3. The lower part of the path integral constructs $e^{-\beta H}$, while the upper part defines the lattice modular T operator, and they glue as indicated to form $Z_{\mathcal{T}} = \mathbf{Tr}(Te^{-\beta H})$. (Periodicity is understood in the x, y directions, so the exposed triangles and the dangling ones in the lattice modular T operator are identified).

invariances remain valid over $\mathcal{T}$. When k is odd, i.e., in fermionic theory, we also need to define z_χ on the special layers. A detailed, systematic approach toward these problems, inspired by [27], can be found in Supplemental Material [13]. And regarding the Maxwell term, we still have it on each plaquette, including the triangular ones. In principle, the Maxwell coupling to be used on those triangular plaquettes is unimportant because it is only going to affect α in Eq. (3). For concreteness, we can make a "uniform" choice with $e^2/2$ in replacement of e^2 on those triangular plaquettes.

Thus, $\langle T \rangle$ is to be evaluated as $Z_{\mathcal{T}}/Z_{\mathrm{T}^3}$; since Z_{T^3} is positive [16], the phase of $\langle T \rangle$ is the phase of $Z_{\mathcal{T}}$.

Setup of calculation—The lattice model [Eq. (4)] (and its fermionic version with z_χ) is defined in a manifestly local manner. But to perform actual calculations, this is not the

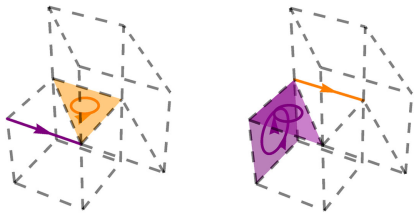


FIG. 4. Left: $(X \cup Y)_c$ for cube c at the lower layer of the lattice T operator receives an extra term in addition to the usual ones in Fig. 2, given by the product of X on the purple link and Y on the orange triangular plaquette. Right: $(Y \cup X)_c$ for cube c at the lower layer of the lattice T operator also receives an extra term: now X on the orange link multiplies not only to Y on the purple square plaquette on the side as usual, but to the sum of Y on both the square and the triangular purple plaquettes.

most convenient form. Rather, it is convenient to exploit the one-form $\mathbb{Z}$ gauge [Eq. (6)] to make A_l $\mathbb{R}$-valued on most links while $s_p = 0$ on most plaquettes. After doing so, the path integral becomes essentially a Gaussian integral, hence solvable, along with some extra treatments that depend manifestly on the spacetime topology—hence the price paid is that this alternative formulation is not manifestly local, but manageable. According to Sec. V and Appendix E of [16], after this procedure, on a spacetime that has no homological torsion—which is applicable to both T^3 and $\mathcal{T}$ (see Supplemental Material [13])—the path integral Z defined by Eq. (4) (or its fermionic version) is equal to Z', where

$$Z' = \left[\prod_l \int_{-\infty}^{\infty} \frac{dA'_l}{2\pi}\right]_{\text{nlocFP}} \times \exp\left\{\frac{ik}{4\pi}\sum_c (A' \cup dA')_c - \frac{1}{2e^2}\sum_p (dA')_p^2\right\} \tag{7}$$

is a Gaussian integral of an $\mathbb{R}$-valued gauge field A'_l, but with an unusual *nonlocal* Faddeev-Popov treatment ("nlocFP"), which does the following: when we perform the Gaussian integral of the $\mathbb{R}$ gauge field, we ignore *any* zero mode of A', i.e., a closed one-form that satisfies $dA' = 0$ regardless of whether the zero mode is an $\mathbb{R}$ gauge transformation (exact one-form, which is indeed removed in the usual Fadeev-Popov procedure, which is local) or a global holonomy (nonexact closed one-form, which is unusual to drop because it is nonlocal to do so). This nlocFP thus removes the diverging size of the one-form $\mathbb{R}$ global symmetry that an actual $\mathbb{R}$ gauge theory would have had [21], rendering the partition function finite, as it should, because the theory really started out as Eq. (4), a manifestly local U(1) rather than $\mathbb{R}$ gauge theory.

After having this alternative expression [Eq. (7)], we can reseparate $\mathcal{T}$ into two parts as in Fig. 3, and interpret the two equivalent expressions [Eq. (4)] (or its fermionic version) and Eq. (7) of the path integral as

$$\mathbf{Tr}\,(Te^{-\beta H}) = Z_{\mathcal{T}} = Z'_{\mathcal{T}} = \mathbf{Tr}(T'e^{-\beta H'}). \tag{8}$$

In this alternative formulation, the lower part of Fig. 3 is constructing $e^{-\beta H'}$ for the $\mathbb{R}$-valued A'. This is a Gaussian integral, and the result is a Gaussian function of those A'_l on the links at the bottom ($\tau = 0$) and top ($\tau = \beta$) boundaries of the path integral. We will present the details in Supplemental Material [13]. Essentially, after Fourier transforming the x and y directions, the Gaussian coefficients in $e^{-\beta H'}$ have an analytical expression that is lengthy; alternatively, their numerical values can be evaluated algorithmically, with time cost scaling as $L^2 \times \log_2 \beta$, where there are L^2 Fourier modes, and the $\log_2 \beta$ is due to iteratively doubling the τ-direction size. For the ground subspace, we will take $\beta \to \infty$.

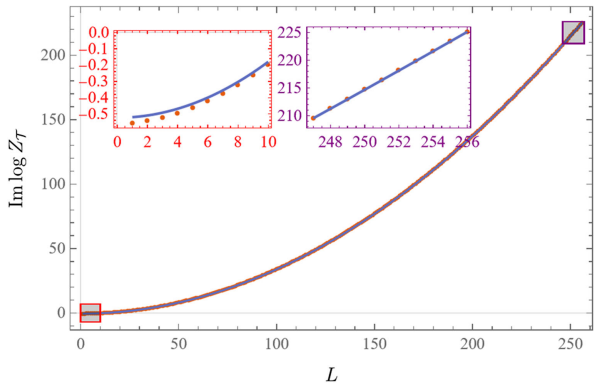


FIG. 5. The orange dots are phases of $Z_{\mathcal{T}}$ for $k = 1$, $e^2 = 1$ at different L's. The blue curve is the quadratic fit using the L's from $L_1 = 129$ to $L_2 = 256$.

On the other hand, the upper part of Fig. 3 is now constructing the modular T operator for the $\mathbb{R}$-valued A', denoted as T'. Because of the complicated lattice in T', although it is still a Gaussian integral, we do not have a closed form expression for the result, so we will algorithmically evaluate the numerical value of the desired $\mathbf{Tr}(T'e^{-\beta H'})$; see Supplemental Material [13]. More exactly, the x direction in the T' part of Fig. 3 can still be Fourier transformed, so only the y direction needs to be handled numerically. The time cost scales as $L \times L^3$, where the L is the number of Fourier modes in the x direction, and, after that, the L^3 arises from the manipulations of matrices in the y coordinates.

Results—Numerical value of the complex phase of the path integral $Z_{\mathcal{T}} = \mathbf{Tr}(Te^{-\beta H}) = \mathbf{Tr}(T'e^{-\beta H'})$ is evaluated using the setup above for various values of k, e^2, and L; since Eq. (4) obviously becomes its complex conjugation upon flipping k, it suffices to consider $k > 0$; and we take $\beta = 2^{12}$, which is sufficiently large to reach the ground subspace. For each value of k and e^2, we fit the phase with the ansatz

$$2\pi C_0 + 2\pi C_2 L^2 \tag{9}$$

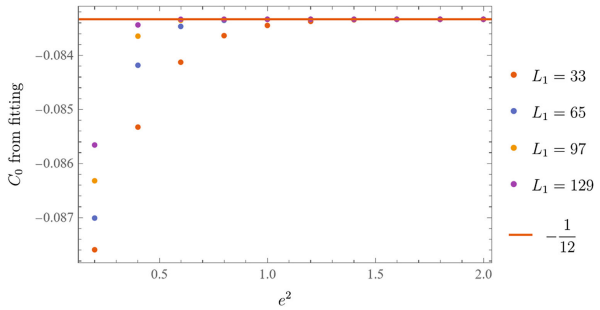


FIG. 6. C_0 fitted using $L_2 = 256$ and increasing values of L_1 and compared to the expected value $-1/12$.

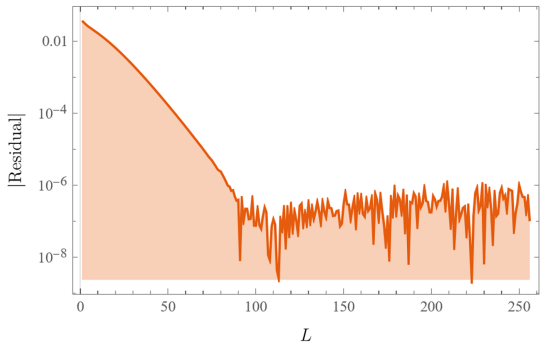


FIG. 7. Deviations of the plotted orange points in Fig. 5 from the blue quadratic fitting curve.

using the L's in a range $L_1 \le L \le L_2$ for some large enough L_1, L_2. Here, C_0 is expected to be $-1/8 + 1/24 = -1/12$ from the universal piece of Eq. (3), and C_2 is from the imaginary part of the nonuniversal α in Eq. (3).

An example of such fit is shown in Fig. 5 and we can see the quadratic ansatz fits well overall. The C_0 fitted for $k = 1$ and different values of e^2, fixing $L_2 = 256$ and using increasing values of L_1, is shown in Fig. 6. As we can see, for larger values of e^2, the fitted C_0 agrees with the desired $-1/12$ very well. Meanwhile, for smaller e^2, there is some deviation when L_1 is small, but the deviation fades away as we increase L_1, the smallest system size used in the fitting. This suggests the deviation is a finite size effect. To confirm this, in Fig. 7 we plot the fitting residual of Fig. 5; alternatively, we can plot the deviation of C_0 from $-1/12$ in Fig. 6 at some fixed e^2 as a function of L_1, and we will get a similar plot. This confirms that the deviation is indeed a finite size effect that vanishes exponentially with L.

Thus, we have confirmed that the evaluated complex phase agrees with the anticipated result [Eq. (3)], with finite size effects vanishing exponentially. We have further confirmed that the magnitude of $Z_{\mathcal{T}}/Z_{\mathrm{T}^3}$, especially its universal part, also agrees with Eq. (3); see Fig. 8.

The code for these computations is available as a separate file.

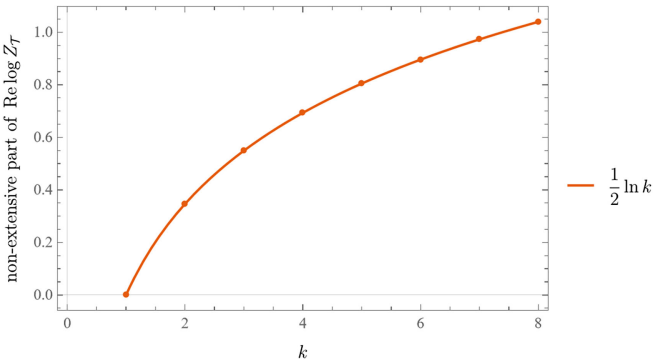


FIG. 8. Numerical result for nonextensive part of Re ln $Z_{\mathcal{T}}$. We set $e^2 = 2$, $L_1 = 129$, $L_2 = 256$, $1 \le k \le 8$.

Conclusion—In this Letter we pinned down the last and perhaps the most crucial property desired for a "successful" realization of U(1) Chern-Simons theory on the lattice [15,16]—the framing anomaly (on top of the other key properties studied in [16]). This not only paints a full picture for the decades-long story of "how to realize U(1) Chern-Simons on the lattice," but also serves as a concrete example of a UV-complete manifestation of a framing anomaly in a way that is different from the ones in which the chirality comes from fermion bands [9].

One immediate and important follow-up question is whether one can also pin down the chiral central charge of the proposed lattice realization of non-Abelian Chern-Simons [17,18], which is necessarily interacting, at least in certain limits.

And it is desirable to cast what we have done in the Hamiltonian formalism. (Note that in the Hamiltonian formalism, there are other interesting ways to realize the modular T operator [28].) The main reason is that it has been fruitful to study chiral central charge through the lens of entanglement [9]—for example, [29,30] showed chiral central charge is a bulk property using the modular commutator instead of framing anomaly, and see, e.g., Refs. [31,32] for more recent developments. We hope our particular construction can be integrated as a concrete example into this general perspective.

Acknowledgments—We appreciate Peng Zhang for the suggestion to evaluate $\langle T^m \rangle$ to extract the full spectrum of T, and Meng Cheng for discussions about the modular T operator in fermionic theories. This work is supported by NSFC under Grants No. 12447104, No. 12174213, and No. 12342501.

Data availability—The data supporting the results in this paper were obtained through the Julia language script available at [33].

[1] A. S. Schwarz, Lett. Math. Phys. **2**, 247 (1978).
[2] E. Witten, Commun. Math. Phys. **121**, 351 (1989).
[3] X.-G. Wen, Adv. Phys. **44**, 405 (1995).
[4] M. Banerjee, M. Heiblum, A. Rosenblatt, Y. Oreg, D. E. Feldman, A. Stern, and V. Umansky, Nature (London) **545**, 75 (2017).
[5] A. Kapustin and L. Spodyneiko, Phys. Rev. B **101**, 045137 (2020).
[6] Q. Niu, D. J. Thouless, and Y.-S. Wu, Phys. Rev. B **31**, 3372 (1985).
[7] E. P. Verlinde, Nucl. Phys. **B300**, 360 (1988).
[8] V. G. Turaev, *Quantum Invariants of Knots and Three Manifolds* (Walter de Gruyter, Berlin and New York, 1994), Vol. 18.
[9] A. Kitaev, Ann. Phys. (Amsterdam) **321**, 2 (2006).
[10] D. Belov and G. W. Moore, arXiv:hep-th/0505235.
[11] M. F. Lapa and M. Levin, Phys. Rev. B **100**, 165129 (2019).

[12] M. Cheng, S. Musser, A. Raz, N. Seiberg, and T. Senthil, Phys. Rev. B **113**, 115103 (2026).
[13] See Supplemental Material at http://link.aps.org/supplemental/10.1103/hyz3-3kxh for details on modular T operators, spacetime topology, lattice cup products, the fermionic path integral, and the numerical evaluation algorithm.
[14] A. Kitaev and L. Kong, Commun. Math. Phys. **313**, 351 (2012).
[15] C. Peng, M. C. Diamantini, L. Funcke, S. M. A. Hassan, K. Jansen, S. Kühn, D. Luo, and P. Naredi, Phys. Rev. D **114**, 034511 (2026).
[16] Z.-A. Xu and J.-Y. Chen, J. High Energy Phys. 08 (2025) 062.
[17] J.-Y. Chen, SciPost Phys. **19**, 158 (2025).
[18] P. Zhang and J.-Y. Chen, J. High Energy Phys. 06 (2025) 085.
[19] S.-H. Ng, A. Schopieray, and Y. Wang, Sel. Math. New Ser. **25**, 53 (2019).
[20] J. Kaidi, Z. Komargodski, K. Ohmori, S. Seifnashri, and S.-H. Shao, SciPost Phys. **13**, 067 (2022).
[21] J.-Y. Chen, Commun. Math. Phys. **381**, 293 (2021).
[22] T. Jacobson and T. Sulejmanpasic, Phys. Rev. D **107**, 125017 (2023).
[23] M. B. Einhorn and R. Savit, Phys. Rev. D **17**, 2583 (1978).
[24] T. Sulejmanpasic and C. Gattringer, Nucl. Phys. **B943**, 114616 (2019).
[25] Z.-C. Gu and X.-G. Wen, Phys. Rev. B **90**, 115141 (2014).
[26] D. Gaiotto and A. Kapustin, Int. J. Mod. Phys. A **31**, 1645044 (2016).
[27] R. G. Thorngren, Combinatorial topology and applications to quantum field theory, Ph.D. thesis, UC, Berkeley (main) (2018).
[28] Y.-Z. You and M. Cheng, arXiv:1502.03192.
[29] I. H. Kim, B. Shi, K. Kato, and V. V. Albert, Phys. Rev. Lett. **128**, 176402 (2022).
[30] I. H. Kim, B. Shi, K. Kato, and V. V. Albert, Phys. Rev. B **106**, 075147 (2022).
[31] X. Li, T.-C. Lin, J. McGreevy, and B. Shi, Phys. Rev. Lett. **134**, 180402 (2025).
[32] X. Li, T.-C. Lin, Y. Alavirad, and J. McGreevy, arXiv:2510.23720.
[33] Z.-A. Xu, Julia code for Framing Anomaly in Lattice Chern-Simons-Maxwell Theory, version 1 (2026), https://arxiv.org/src/2601.04318v1/anc/chern_simons_calculation.jl.

End Matter

As we mentioned in the introduction, to extract the full spectrum of T, we shall evaluate the lattice version of $\langle T^m \rangle$. It is realized as $Z_{\mathcal{T}_m}/Z_{\mathrm{T}^3}$, where $Z_{\mathcal{T}_m} = \mathbf{Tr}((Te^{-\beta H/m})^m)$, with $\mathcal{T}_m$ the closed manifold obtained by having m copies of Fig. 3, such that the top square grid of each T is now glued to the bottom square grid of its next $e^{-\beta H/m}$—obviously, the "next of the mth copy" is the first. Note that unlike the $m = 1$ case, in $\mathcal{T}_m$, a loop across the x direction has nontrivial $\mathbb{Z}_m$ homological torsion, i.e., such a loop is noncontractible, but running around it m times becomes contractible; see Supplemental Material [13]. [Note that if T exactly commutes with H, then $\mathbf{Tr}((Te^{-\beta H/m})^m) = \mathbf{Tr}(T^m e^{-\beta H})$, but now we do not expect this to exactly hold in the lattice realization, so each $e^{-\beta H/m}$ in between two T's, with large enough β, is to relax the system back to the ground subspace after each T operation.]

For further numerical calculation, similar to the case of $Z_{\mathcal{T}}$, we relate $Z_{\mathcal{T}_m}$ to the path integral $Z'_{\mathcal{T}_m}$ of an $\mathbb{R}$ gauge field. According to Appendix E of [16], we have

$$Z_{\mathcal{T}_m} = Z'_{\mathcal{T}_m} \sum_{j=0}^{m-1} e^{i\pi k j^2/m} (-1)^{kj}. \tag{A1}$$

Here, the appearance of an additional factor [compared to Eq. (8)] is due to the extra $\mathbb{Z}_m$ torsion of a loop running across the x direction. [For odd k fermionic theories, recall T is only defined if the fermions are periodic across the x direction, and Eq. (A1) is valid for this case. If the fermions are antiperiodic across the x direction, we can nonetheless still define T^m for even m; see Supplemental Material [13], and in this case we have Eq. (A1) but with the $(-1)^{kj}$ factor

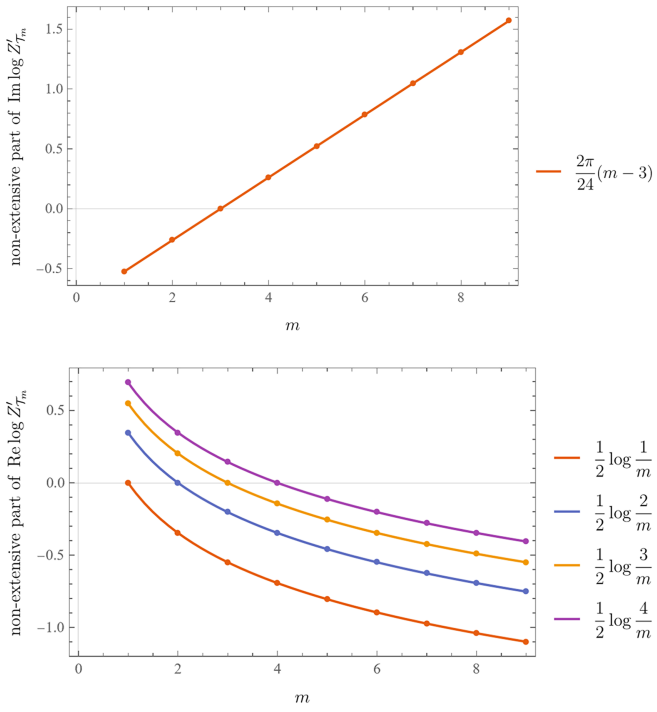


FIG. 9. Numerical results for the nonextensive parts of Im $\ln Z'_{\mathcal{T}_m}$ and Re $\ln Z'_{\mathcal{T}_m}$. We set $e^2 = 2$, $L_1 = 129$, $L_2 = 256$, $1 \le m \le 9$, and $k = 1$ in the upper panel (the result is actually independent of $|k|$) and $1 \le k \le 4$ in the lower panel.

removed.] So, still, our remaining task is to evaluate Eq. (7), now decomposed as $Z'_{\mathcal{T}_m} = \mathbf{Tr}((T' e^{-\beta H'/m})^m)$.

Before proceeding with the numerical computation, let us first explain what we shall expect for the $Z'_{\mathcal{T}_m}$ to be evaluated. We use the following facts: for even k,

$$\frac{1}{\sqrt{|k|}} \sum_{n=0}^{|k|-1} e^{-i\pi \frac{m}{k} n^2} = e^{-i2\pi\, \mathrm{sgn} k/8} \frac{1}{\sqrt{m}} \sum_{j=0}^{m-1} e^{i\pi \frac{k}{m} j^2}, \tag{A2}$$

and for odd k,

$$\frac{1}{\sqrt{|k|}} \sum_{n=0}^{|k|-1} e^{-i\pi \frac{m}{k}(n+1/2)^2} = e^{-i2\pi\, \mathrm{sgn} k/8} \frac{1}{\sqrt{m}} \sum_{j=0}^{m-1} e^{i\pi \frac{k+m}{m} j^2}. \tag{A3}$$

Here, the left-hand sides are the anticipated h_n contributions in Eq. (1). Comparing the right-hand sides to Eq. (A1), what we shall anticipate would be

$$Z'_{\mathcal{T}_m} = \sqrt{\frac{|k|}{m}} e^{-i2\pi\, \mathrm{sgn} k(1/8 - m/24)} e^{-\epsilon_0 \beta L^2 - m\alpha L^2 + \cdots}. \tag{A4}$$

[For odd k fermionic theories, recall the fermions must be periodic across the x direction for T to be defined. However, if we consider T^m with even m only, we can also allow the antiperiodic situation, in which case the $+1/2$ modification will be removed (see Supplemental Material [13]), but the $(-1)^{kj}$ in Eq. (A1) is also removed, resulting in the same anticipation for $Z'_{\mathcal{T}_m}$.] The numerical procedure for $m = 1$ can now be applied to generic m. We indeed obtain the anticipated form of $Z'_{\mathcal{T}_m}$ (see Fig. 9), thus confirming the anticipated full spectrum of T in the lattice Chern-Simons theory.